

Hot neutron star in generalized thermo-statistics

K. Miyazaki

E-mail: miyazakiro@rio.odn.ne.jp

Abstract

The hot neutron star (NS) is investigated for the first time in the generalized thermo-statistics so as to take into account the breaking of the standard Boltzmann-Gibbs thermo-statistics under the long-ranged gravitational potential. It is found that at sub-saturation density in hot NS matter the gravitation leads to a stiffer equation of state than the standard thermo-statistics. The hot NSs in the generalized thermo-statistics are therefore much more massive and larger than those in the standard thermo-statistics.

The study of neutron star (NS) is an important subject in nuclear physics and astrophysics. The equation of state (EOS) of NS matter is developed [1-3] in a microscopic nuclear model of highly dense and asymmetric nuclear matter. Then, the EOS is applied to Einstein equation or Tolman-Oppenheimer-Volkov equation [4] for non-magnetized and non-rotating NS. We distinguish the local microscopic physics from the global macroscopic physics. There is no correlation between the two physics because the gravitation can be neglected as compared with nuclear force. The complete separation of the local and global pictures is really reasonable for cold NS, while it does not necessarily succeed in hot NS encountered during the evolution [5,6] of proto-neutron star. Although the gravitation does not play an explicit role in nuclear EOS, it may have an implicit effect on the EOS through the breaking of the standard Boltzmann-Gibbs thermo-statistics under the long-ranged potential.

In fact, it is recently shown in the analysis [7] of the temperature fluctuations of cosmic microwave background that the generalized thermo-statistics [8-10] is really satisfactory under gravitational potential. The present paper therefore calculates for the first time the EOS of hot NS in the generalized thermo-statistics in contrast to the preceding papers [11-16] that assumed a priori the validity of the standard thermo-statistics under gravitational potential. Here, we easily expect that the effect of gravitation on the EOS is taken into account implicitly through the phenomenological power-law index although the theoretical derivation of the index is a subject of future investigations.

In this work we make use of the relativistic mean-field (RMF) model of nuclear matter developed in Ref. [16]. The RMF model is reasonable for NS matter because the general

relativity is based on the validity of special relativity at local space-time, where the microscopic nuclear model is developed. We extend the thermodynamic potential in Ref. [16] using the q -deformed exponential and logarithm:

$$\exp_q(x) \equiv [1 + (1 - q)x]^{1/(1-q)}, \quad (1)$$

$$\ln_q(x) \equiv \frac{x^{1-q} - 1}{1 - q}. \quad (2)$$

Consequently, the thermodynamic potential Ω_q in the generalized thermo-statistics is

$$\begin{aligned} \Omega_q = & \frac{1}{2} m_\sigma^2 \langle \sigma \rangle^2 + \frac{1}{2} m_\delta^2 \langle \delta_3 \rangle^2 + \frac{1}{2} m_{\sigma^*}^2 \langle \sigma^* \rangle^2 - \frac{1}{2} m_\omega^2 \langle \omega_0 \rangle^2 - \frac{1}{2} m_\rho^2 \langle \rho_{03} \rangle^2 - \frac{1}{2} m_\phi^2 \langle \phi_0 \rangle^2 \\ & - 2 k_B T \sum_{\substack{B=p,n,\Lambda,\Sigma^+, \\ \Sigma^0, \Sigma^-, \Xi^0, \Xi^-}} \int \frac{d^3 \mathbf{k}}{(2\pi)^3} \left\{ \ln_q \left[1 + \exp_q \left(\frac{\nu_B - E_{kB}^*}{k_B T} \right) \right] \right. \\ & \quad \left. + \ln_q \left[1 + \exp_q \left(\frac{-\nu_B - E_{kB}^*}{k_B T} \right) \right] \right\} \\ & - 2 k_B T \sum_{l=e^-, \mu^-} \int \frac{d^3 \mathbf{k}}{(2\pi)^3} \left\{ \ln_q \left[1 + \exp_q \left(\frac{\mu_l - e_{kl}}{k_B T} \right) \right] \right. \\ & \quad \left. + \ln_q \left[1 + \exp_q \left(\frac{-\mu_l - e_{kl}}{k_B T} \right) \right] \right\}, \quad (3) \end{aligned}$$

where k_B is the Boltzmann constant and ν_B is given by the chemical potential μ_B and the vector potential V_B of baryon as

$$\nu_B = \mu_B - V_B. \quad (4)$$

$M_B^* = m_B^* M_B$ and $E_{kB}^* = (\mathbf{k}^2 + M_B^{*2})^{1/2}$ are the effective mass and the energy of baryon while μ_l and $e_{kl} = (\mathbf{k}^2 + m_l^2)^{1/2}$ are the chemical potential and the energy of lepton.

The scalar mean-fields $\langle \sigma \rangle$, $\langle \delta_3 \rangle$ and $\langle \sigma^* \rangle$ in Eq. (3) are expressed [16] in terms of three independent effective masses of p , n and Λ while the vector mean-fields $\langle \omega_0 \rangle$, $\langle \rho_{03} \rangle$ and $\langle \phi_0 \rangle$ are expressed [16] in terms of three independent vector potentials of p , n and Λ . Then, M_p^* , M_n^* , M_Λ^* , V_p , V_n and V_Λ are determined from extremizing the thermodynamic potential Ω_q in terms of them. The results are

$$\begin{aligned} \rho_p + \sum_{Y \neq \Lambda} \frac{g_{YY\omega}^* g_{nn\rho}^* + I_{3Y} g_{YY\rho}^* g_{nn\omega}^* - (g_{\Lambda\Lambda\omega}^*/g_{\Lambda\Lambda\phi}^*) g_{YY\phi}^* g_{nn\rho}^*}{g_{pp\omega}^* g_{nn\rho}^* + g_{nn\omega}^* g_{pp\rho}^*} \rho_Y \\ - \frac{g_{nn\rho}^* m_\omega^2 \langle \omega_0 \rangle + g_{nn\omega}^* m_\rho^2 \langle \rho_{03} \rangle - (g_{\Lambda\Lambda\omega}^*/g_{\Lambda\Lambda\phi}^*) g_{nn\rho}^* m_\phi^2 \langle \phi_0 \rangle}{g_{pp\omega}^* g_{nn\rho}^* + g_{nn\omega}^* g_{pp\rho}^*} = 0, \quad (5) \end{aligned}$$

$$\rho_n + \sum_{Y \neq \Lambda} \frac{g_{Y\omega}^* g_{pp\rho}^* - I_{3Y} g_{Y\rho}^* g_{pp\omega}^* - (g_{\Lambda\Lambda\omega}^*/g_{\Lambda\Lambda\phi}^*) g_{Y\phi}^* g_{pp\rho}^*}{g_{pp\omega}^* g_{nn\rho}^* + g_{nn\omega}^* g_{pp\rho}^*} \rho_Y - \frac{g_{pp\rho}^* m_\omega^2 \langle \omega_0 \rangle - g_{pp\omega}^* m_\rho^2 \langle \rho_{03} \rangle - (g_{\Lambda\Lambda\omega}^*/g_{\Lambda\Lambda\phi}^*) g_{pp\rho}^* m_\phi^2 \langle \phi_0 \rangle}{g_{pp\omega}^* g_{nn\rho}^* + g_{nn\omega}^* g_{pp\rho}^*} = 0, \quad (6)$$

$$\rho_\Lambda + \sum_{Y \neq \Lambda} \frac{g_{Y\phi}^*}{g_{\Lambda\Lambda\phi}^*} \rho_Y - \left(\frac{m_\phi}{g_{\Lambda\Lambda\phi}^*} \right)^2 (V_\Lambda - g_{\Lambda\Lambda\omega}^* \langle \omega_0 \rangle) = 0, \quad (7)$$

$$M_p \rho_{pS} + \sum_{Y \neq \Lambda} \frac{\partial m_Y^*}{\partial m_p^*} M_Y \rho_{YS} + \sum_{Y \neq \Lambda} \frac{\partial V_Y}{\partial m_p^*} \rho_Y + m_\sigma^2 \langle \sigma \rangle \frac{\partial \langle \sigma \rangle}{\partial m_p^*} + m_\delta^2 \langle \delta_3 \rangle \frac{\partial \langle \delta_3 \rangle}{\partial m_p^*} + m_{\sigma^*}^2 \langle \sigma^* \rangle \frac{\partial \langle \sigma^* \rangle}{\partial m_p^*} - m_\omega^2 \langle \omega_0 \rangle \frac{\partial \langle \omega_0 \rangle}{\partial m_p^*} - m_\rho^2 \langle \rho_{03} \rangle \frac{\partial \langle \rho_{03} \rangle}{\partial m_p^*} - m_\phi^2 \langle \phi_0 \rangle \frac{\partial \langle \phi_0 \rangle}{\partial m_p^*} = 0, \quad (8)$$

$$M_n \rho_{nS} + \sum_{Y \neq \Lambda} \frac{\partial m_Y^*}{\partial m_n^*} M_Y \rho_{YS} + \sum_{Y \neq \Lambda} \frac{\partial V_Y}{\partial m_n^*} \rho_Y + m_\sigma^2 \langle \sigma \rangle \frac{\partial \langle \sigma \rangle}{\partial m_n^*} + m_\delta^2 \langle \delta_3 \rangle \frac{\partial \langle \delta_3 \rangle}{\partial m_n^*} + m_{\sigma^*}^2 \langle \sigma^* \rangle \frac{\partial \langle \sigma^* \rangle}{\partial m_n^*} - m_\omega^2 \langle \omega_0 \rangle \frac{\partial \langle \omega_0 \rangle}{\partial m_n^*} - m_\rho^2 \langle \rho_{03} \rangle \frac{\partial \langle \rho_{03} \rangle}{\partial m_n^*} - m_\phi^2 \langle \phi_0 \rangle \frac{\partial \langle \phi_0 \rangle}{\partial m_n^*} = 0, \quad (9)$$

$$M_\Lambda \rho_{\Lambda S} + \sum_{Y \neq \Lambda} \frac{\partial m_Y^*}{\partial m_\Lambda^*} M_Y \rho_{YS} + \sum_{Y \neq \Lambda} \frac{\partial V_Y}{\partial m_\Lambda^*} \rho_Y + m_{\sigma^*}^2 \langle \sigma^* \rangle \frac{\partial \langle \sigma^* \rangle}{\partial m_\Lambda^*} - m_\phi^2 \langle \phi_0 \rangle \frac{\partial \langle \phi_0 \rangle}{\partial m_\Lambda^*} = 0. \quad (10)$$

I_{3Y} is the isospin of hyperon. The effective coupling constants $g_{BB\sigma}^*$ etc. are defined in Ref. [16]. For the free meson-baryon coupling constants $g_{BB\sigma}$ etc. we make use of the EZM-P model of Table 1 in Ref. [17]. The calculations of the derivatives in Eqs. (5)-(10) are tedious but straightforward tasks and so their explicit expressions are not shown.

The baryon density is defined [18] by

$$\rho_B = -\frac{\partial \Omega_q}{\partial \mu_B} = 2 \int \frac{d^3 \mathbf{k}}{(2\pi)^3} [(n_{qB}(k))^q - (\bar{n}_{qB}(k))^q], \quad (11)$$

where the q -deformed Fermi-Dirac distribution functions [18] are

$$\begin{bmatrix} n_{qB}(k) \\ \bar{n}_{qB}(k) \end{bmatrix} = \begin{cases} \frac{1}{1 + \left[1 + (q-1) \frac{E_{kB}^* \mp \nu_B}{k_B T} \right]^{\frac{1}{q-1}}} & \text{for } 1 + (q-1) \frac{E_{kB}^* \mp \nu_B}{k_B T} > 0 \\ 1 & \text{for } 1 + (q-1) \frac{E_{kB}^* \mp \nu_B}{k_B T} \leq 0 \end{cases}. \quad (12)$$

The upper and lower signs are for baryon and anti-baryon, respectively. Similarly, the lepton density is defined by

$$\rho_l = -\frac{\partial \Omega_q}{\partial \mu_l} = 2 \int \frac{d^3 \mathbf{k}}{(2\pi)^3} [(n_{ql}(k))^q - (\bar{n}_{ql}(k))^q], \quad (13)$$

where

$$\begin{bmatrix} n_{ql}(k) \\ \bar{n}_{ql}(k) \end{bmatrix} = \begin{cases} \frac{1}{1 + \left[1 + (q-1) \frac{e_{kl} \mp \mu_l}{k_B T}\right]^{\frac{1}{q-1}}} & \text{for } 1 + (q-1) \frac{e_{kl} \mp \mu_l}{k_B T} > 0 \\ 1 & \text{for } 1 + (q-1) \frac{e_{kl} \mp \mu_l}{k_B T} \leq 0 \end{cases}. \quad (14)$$

The scalar density of baryon is defined [18] by

$$\rho_{BS} = 2 \int \frac{d^3 \mathbf{k}}{(2\pi)^3} \frac{M_B^*}{E_{kB}^*} [(n_{qB}(k))^q + (\bar{n}_{qB}(k))^q]. \quad (15)$$

The entropy is calculated [18] as

$$\begin{aligned} TS &= -T \frac{\partial \Omega_q}{\partial T} \\ &= \frac{1}{2} m_\sigma^2 \langle \sigma \rangle^2 + \frac{1}{2} m_\delta^2 \langle \delta_3 \rangle^2 + \frac{1}{2} m_{\sigma^*}^2 \langle \sigma^* \rangle^2 \\ &\quad - \frac{1}{2} m_\omega^2 \langle \omega_0 \rangle^2 - \frac{1}{2} m_\rho^2 \langle \rho_{03} \rangle^2 - \frac{1}{2} m_\phi^2 \langle \phi_0 \rangle^2 - \Omega_q \\ &\quad - \sum_{\substack{B=p,n,\Lambda,\Sigma^+, \\ \Sigma^0,\Sigma^-, \Xi^0,\Xi^-}} (\mu_B - V_B) \rho_B + 2 \sum_{\substack{B=p,n,\Lambda,\Sigma^+, \\ \Sigma^0,\Sigma^-, \Xi^0,\Xi^-}} \int \frac{d^3 \mathbf{k}}{(2\pi)^3} E_{kB}^* [(n_{qB}(k))^q + (\bar{n}_{qB}(k))^q] \\ &\quad - \sum_{l=e^-, \mu^-} \mu_l \rho_l + 2 \sum_{l=e^-, \mu^-} \int \frac{d^3 \mathbf{k}}{(2\pi)^3} e_{kl} [(n_{ql}(k))^q + (\bar{n}_{ql}(k))^q]. \end{aligned} \quad (16)$$

If the energy density is defined by

$$\begin{aligned} \mathcal{E} &= \frac{1}{2} m_\sigma^2 \langle \sigma \rangle^2 + \frac{1}{2} m_\delta^2 \langle \delta_3 \rangle^2 + \frac{1}{2} m_{\sigma^*}^2 \langle \sigma^* \rangle^2 - \frac{1}{2} m_\omega^2 \langle \omega_0 \rangle^2 - \frac{1}{2} m_\rho^2 \langle \rho_{03} \rangle^2 - \frac{1}{2} m_\phi^2 \langle \phi_0 \rangle^2 \\ &\quad + 2 \sum_{\substack{B=p,n,\Lambda,\Sigma^+, \\ \Sigma^0,\Sigma^-, \Xi^0,\Xi^-}} \left\{ \left(\int \frac{d^3 \mathbf{k}}{(2\pi)^3} E_{kB}^* [(n_{qB}(k))^q + (\bar{n}_{qB}(k))^q] \right) + V_B \rho_B \right\} \\ &\quad + 2 \sum_{l=e^-, \mu^-} \int \frac{d^3 \mathbf{k}}{(2\pi)^3} e_{kl} [(n_{ql}(k))^q + (\bar{n}_{ql}(k))^q], \end{aligned} \quad (17)$$

Eq. (16) is just the thermodynamic relation:

$$\Omega_q = \mathcal{E} - T S - \sum_{\substack{i=p,n,\Lambda,\Sigma^+,\Sigma^0, \\ \Sigma^-, \Xi^0, \Xi^-, e^-, \mu^-}} \mu_i \rho_i. \quad (18)$$

So as to obtain the normal expression of pressure

$$\begin{aligned} P &= -\Omega_q = \frac{2}{3} \sum_{\substack{B=p,n,\Lambda,\Sigma^+, \\ \Sigma^0, \Sigma^-, \Xi^0, \Xi^-}} \int \frac{d^3\mathbf{k}}{(2\pi)^3} \frac{k^2}{E_{kB}^*} [(n_{qB}(k))^q + (\bar{n}_{qB}(k))^q] \\ &+ \frac{2}{3} \sum_{l=e^-, \mu^-} \int \frac{d^3\mathbf{k}}{(2\pi)^3} \frac{k^2}{e_{kl}} [(n_{ql}(k))^q + (\bar{n}_{ql}(k))^q] \\ &- \frac{1}{2} m_\sigma^2 \langle \sigma \rangle^2 - \frac{1}{2} m_\delta^2 \langle \delta_3 \rangle^2 - \frac{1}{2} m_{\sigma^*}^2 \langle \sigma^* \rangle^2 + \frac{1}{2} m_\omega^2 \langle \omega_0 \rangle^2 + \frac{1}{2} m_\rho^2 \langle \rho_{03} \rangle^2 + \frac{1}{2} m_\phi^2 \langle \phi_0 \rangle^2, \end{aligned} \quad (19)$$

the power-law index has to satisfy the condition [18]:

$$1 < q < 4/3. \quad (20)$$

The deformed Fermi integrals in Eqs. (11), (13), (15), (17) and (19) are transformed to the integrals in finite ranges by converting the variable k into $1/E_{kB}^*$ and $1/e_{kl}$. They are calculated using the adaptive automatic integration with 20-points Gaussian quadrature. The condition (20) also guarantees finite values of the integrals.

In our model the leptons are treated as the free Fermi gases. They however couple to baryons through the chemical equilibrium condition

$$\mu_i = b_i \mu_n - q_i \mu_{e^-}, \quad (21)$$

and the charge neutral condition

$$\sum_{\substack{i=p,n,\Lambda,\Sigma^+,\Sigma^0, \\ \Sigma^-, \Xi^0, \Xi^-, e^-, \mu^-}} q_i \rho_i = 0, \quad (22)$$

where b_i and q_i are baryon number and charge of each particle. Then, we solve 8-rank non-linear simultaneous equations of (5)-(10), (22) and the baryon number conservation

$$\rho_T = \sum_{\substack{B=p,n,\Lambda,\Sigma^+, \\ \Sigma^0, \Sigma^-, \Xi^0, \Xi^-}} \rho_B, \quad (23)$$

so that M_p^* , M_n^* , M_Λ^* , V_p , V_n , V_Λ , μ_n and μ_{e^-} are determined. Using them the energy density (17) and the pressure density (19) are calculated. The results are the inputs to

Tolman-Oppenheimer-Volkov equation [4]:

$$\frac{dM_G(r)}{dr} = \frac{4\pi^2}{c^2} r^2 \mathcal{E}(r), \quad (24)$$

$$\frac{dP(r)}{dr} = -\frac{G}{c^2} \frac{[\mathcal{E}(r) + P(r)] [M_G(r) + 4\pi r^3 P(r)/c^2]}{r [r - 2GM_G(r)/c^2]}. \quad (25)$$

$P(r)$, $\mathcal{E}(r)$ and $M_G(r)$ are the radial distributions of pressure, energy and gravitational mass in NS.

Figures 1, 2, 3 and 4 show particle fractions in the cores of hot NSs at $T = 20\text{MeV}$ for $q = 1.0, 1.1, 1.2$ and 1.3 , respectively. Figure 1 is just the result in the standard Boltzmann-Gibbs thermo-statistics. Here, Λ appears first among all the hyperons because it is the lightest one and because its potential in the saturated nuclear matter is assumed to be most attractive. (See Eq. (54) in Ref. [17].) Next, Ξ^- appears because it is negatively charged and because the potential of Ξ is also assumed to be attractive. Ξ^0 appears later than Σ^- because Ξ^0 has no charge and is heavier than Σ^- . Σ^- is however much poorer than Ξ^0 and Ξ^- at high densities because the potential of Σ in the saturated nuclear matter is assumed to be repulsive. Σ^0 and Σ^+ do not appear because they are neutral and positively charged. As the power-law index increases to $q = 1.1$, Λ appears in the whole range of total baryon density, while Σ^- appears above $\rho_T = 0.2\text{fm}^{-3}$ and below $\rho_T = 0.1\text{fm}^{-3}$. As the power-law index increases further to $q = 1.2$, Σ^0 and Σ^- appear in the whole range of density, while Σ^+ appears below $\rho_T = 0.1\text{fm}^{-3}$. As the power-law index increases extremely to $q = 1.3$, all the hyperons appear in the whole range of density.

In the inner core of hot NS, even for $q = 1.3$ the fractions of hyperons are essentially controlled by their potentials in the saturated nuclear matter defined in terms of Eq. (54) in Ref. [17]. On the other hand, the nucleon fractions at $\rho_T = 1.0\text{fm}^{-3}$ are almost constant in Figs. 1, 2, 3 and 4. The results indicate that the total strangeness fraction in an inner core of hot NS is almost independent on the power-law index. Therefore, even in Fig. 4 we do not find the softening of nuclear EOS owing to an abundance of strangeness. Consequently, the stiffness of EOS in the inner core does not depend strongly on the power-law index. The result is reasonable because at high baryon densities the implicit effect of gravitation on the EOS through the power-law index would be much weaker than the effect of nuclear interaction.

We can see in Figs. 2, 3 and 4 that at sub-saturation densities below $\rho_T = 0.16\text{fm}^{-3}$ the thermal effect becomes more and more dominant over the effect of nuclear interactions with the power-law index increasing. Here, the baryon mass plays a major role to determine baryon fraction while the baryon charge plays a supplementary role. The lightest Λ is most abundant among all the hyperons. Then, the negatively charged Σ^- is more abundant than neutral Σ^0 . The heavier but negatively charged Ξ^- is more abun-

dant than the lighter but positively charged Σ^+ . Ξ^0 is the poorest because of its charge neutrality and heavier mass than Σ^+ .

Next, we assume that the NS has a hot core in the region $\rho_T \geq 0.1\text{fm}^{-3}$ but a cold crust in the region $\rho_T < 10^{-3}\text{fm}^{-3}$. For the former the EOS of our model is applied while for the latter we make use of the EOSs by Feynman-Metropolis-Teller, Baym-Pethick-Sutherland and Negele-Vautherin in Ref. [19]. The EOS between the two regions is obtained from simple linear interpolation. Figure 5 shows for $q = 1.0, 1.1, 1.2, 1.25$ and 1.3 the gravitational masses of NSs at $T = 20\text{MeV}$ as functions of radius. The most massive NSs lie almost on the dotted line. Their gravitational masses are $M_G = 1.606M_\odot, 1.614M_\odot, 1.638M_\odot, 1.674M_\odot$ and $1.814M_\odot$, respectively. Their radii are $R = 14.68\text{km}, 14.92\text{km}, 15.44\text{km}, 16.12\text{km}$ and 18.33km , respectively. It is seen that a higher value of the power-law index predicts a more massive and larger NS.

As seen above, the power-law index does not have a strong effect on the EOS in an inner core of NS, while a larger value of the index produces the stronger thermal pressure below the saturation density $\rho_T = 0.16\text{fm}^{-3}$. The result in Fig. 5 is therefore due to the stiffer EOS just above $\rho_T = 0.1\text{fm}^{-3}$ with the power-law index increasing. At lower baryon density, because the effect of nuclear interaction on nuclear EOS is weaker, we can expect that the implicit effect of gravitation through the power-law index is oppositely stronger. The stiffer EOS just above $\rho_T = 0.1\text{fm}^{-3}$ is therefore due to the stronger effect of gravitation from a larger value of the power-law index. Consequently, we can see that the result in Fig. 5 shows the effect of gravitation on nuclear EOS.

The effect of the generalized thermo-statistics is more remarkable in Fig. 6, which shows the gravitational masses of NSs at a higher temperature $T = 30\text{MeV}$ than Fig. 5. The masses of the most massive NSs are $M_G = 1.658M_\odot, 1.698M_\odot, 1.834M_\odot, 2.218M_\odot$ and $3.106M_\odot$, respectively. Their radii are $R = 15.83\text{km}, 16.60\text{km}, 18.83\text{km}, 27.05\text{km}$ and 27.51km , respectively. Below $q = 1.25$ the most massive NSs also lie on the dotted line, while above $q = 1.25$ their radii are almost constant. At a higher temperature, because the effect of nuclear interaction on nuclear EOS is weaker, we can expect that the effect of gravitation through the power-law index is oppositely stronger. Consequently, the much larger effect of power-law index in Fig. 6 than Fig. 5 shows that the gravitation really has an effect on nuclear EOS in the generalized thermo-statistics, although Fig. 6 only shows numerical experiments that are not physically realized.

We have calculated for the first time the hot NS in the generalized thermo-statistics. It has been found that as compared with the standard Boltzmann-Gibbs thermo-statistics, the generalized one increases the thermal pressure and so leads to a stiffer EOS at sub-saturation density in NS matter. Consequently, a power-law index $q = 1.3$ predicts much more massive and larger NSs than $q = 1.0$ of the standard thermo-statistics. If the power-law index decreases during the cooling of hot NS, the black hole would be born. Although we have introduced the generalized thermo-statistics so as to take into account the breaking of the standard thermo-statistics under the long-ranged gravitational po-

tential, the physical mechanism of $q > 1$ due to gravitation is not known at present. The study of the mechanism is a challenging subject of future works.

References

- [1] J.M. Lattimer and M. Prakash, *Science* **304** (2004) 536 [arXiv:astro-ph/0405262].
- [2] J.M. Lattimer and M. Prakash, *Phys. Rep.* **442** (2007) 109 [arXiv:astro-ph/0612440].
- [3] F. Weber, R. Negreiros and P. Rosenfield, arXiv:astro-ph/0705.2708.
- [4] W.D. Arnett and R.L. Bowers, *Astrophys. J. Suppl.* **33** (1977) 415.
- [5] M. Prakash, I. Bombaci, M. Prakash, P.J. Ellis, R. Knorren and J.M. Lattimer, *Phys. Rep.* **280** (1997) 1, [arXiv:nucl-th/9603042].
- [6] M. Prakash, J.M. Lattimer, J.A. Pons, A.W. Steiner and S. Reddy, *Lect. Notes Phys.* **578** (2001) 364 [arXiv:astro-ph/0012136].
- [7] A. Bernui, C. Tsallis and T. Villela, *Eur. Phys. Lett.* **78** (2007) 19001 [arXiv:astro-ph/0703708].
- [8] C. Tsallis, *Braz. J. Phys.* **29** (1999) 1.
- [9] *Europhysics News* **36** (2005) No.6 [http://www.europhysicsnews.com].
- [10] C. Tsallis, <http://tsallis.cat.cbpf.br/TEMUCO3.pdf>.
- [11] K. Strobel, Ch. Schaab and M.K. Weigel, *Astron. Astrophys.* **350** (1999) 497.
- [12] R. Mańka, M. Zastawny-Kubica, A. Brzezina and I. Bednarek, *J. Phys. G* **27** (2001) 1917 [arXiv:astro-ph/0012088].
- [13] G.F. Marranghello, C.A.Z. Vasconcellos, M. Dillig and J.A. De F. Pacheco, *Int. J. Mod. Phys. E* **11** (2002) 83. [arXiv:astro-ph/0107476].
- [14] D.P. Menezes and C. Providência, *Phys. Rev. C* **69** (2004) 045801 [arXiv:nucl-th/0312050].
- [15] O.E. Nicotra, M. Baldo, G.F. Burgio and H.-J. Schulze, *Astron. Astrophys.* **451** (2006) 213 [arXiv:nucl-th/0506066].
- [16] K. Miyazaki, *Mathematical Physics Preprint Archive* (mp_arc) 05-427.
- [17] K. Miyazaki, *Mathematical Physics Preprint Archive* (mp_arc) 06-175.
- [18] K. Miyazaki, *Mathematical Physics Preprint Archive* (mp_arc) 07-92.
- [19] V. Canuto, *Ann. Rev. Astr. Ap.* **12** (1974) 167; **13** (1975) 335.

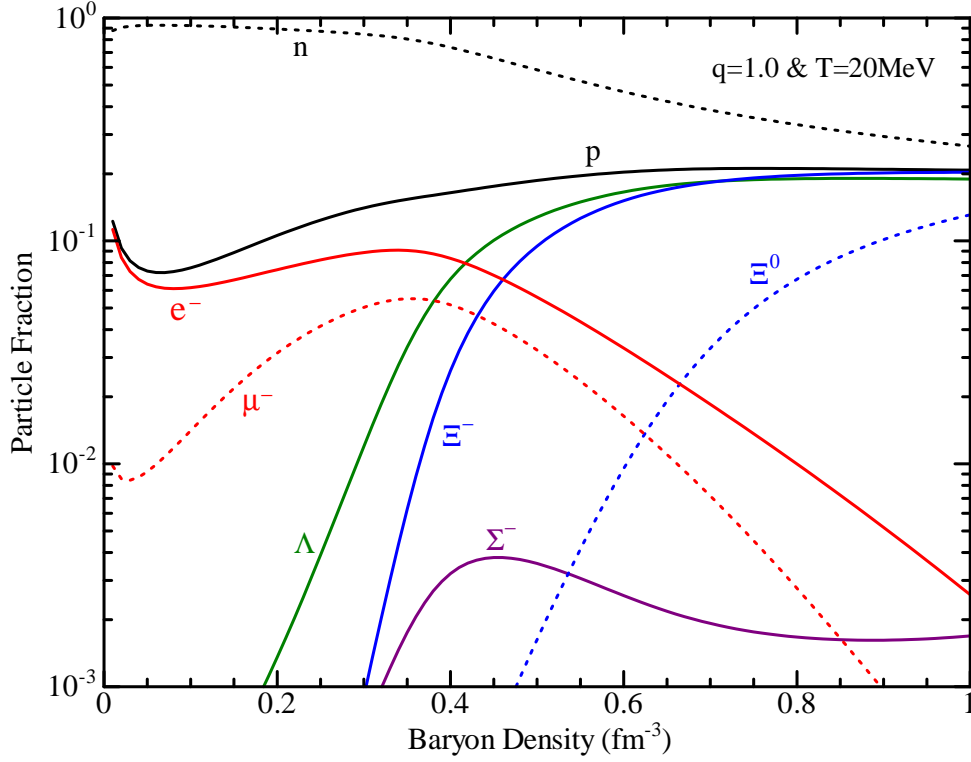


Figure 1: The particle fractions in the core of hot NS at $T = 20 \text{ MeV}$ in the standard Boltzmann-Gibbs thermo-statistics.

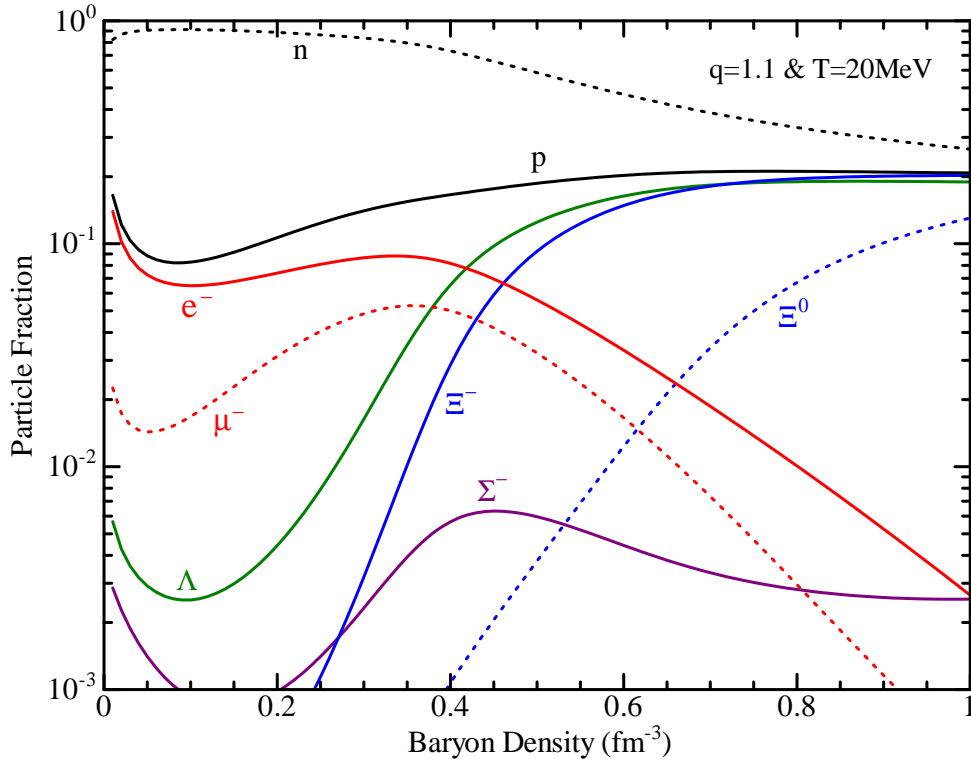
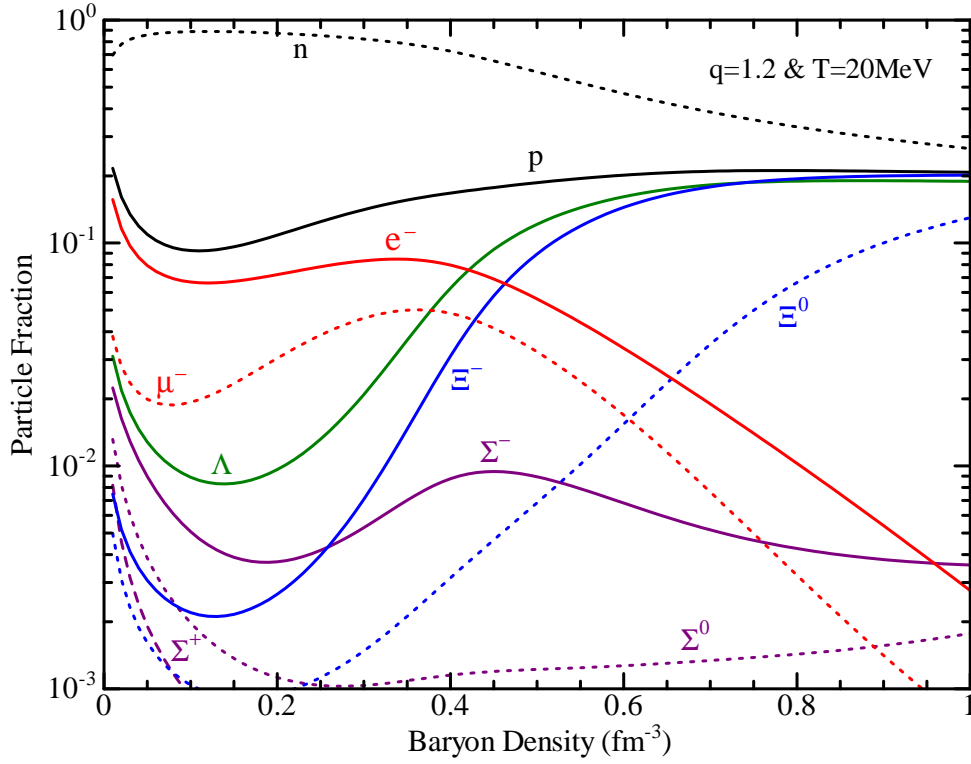
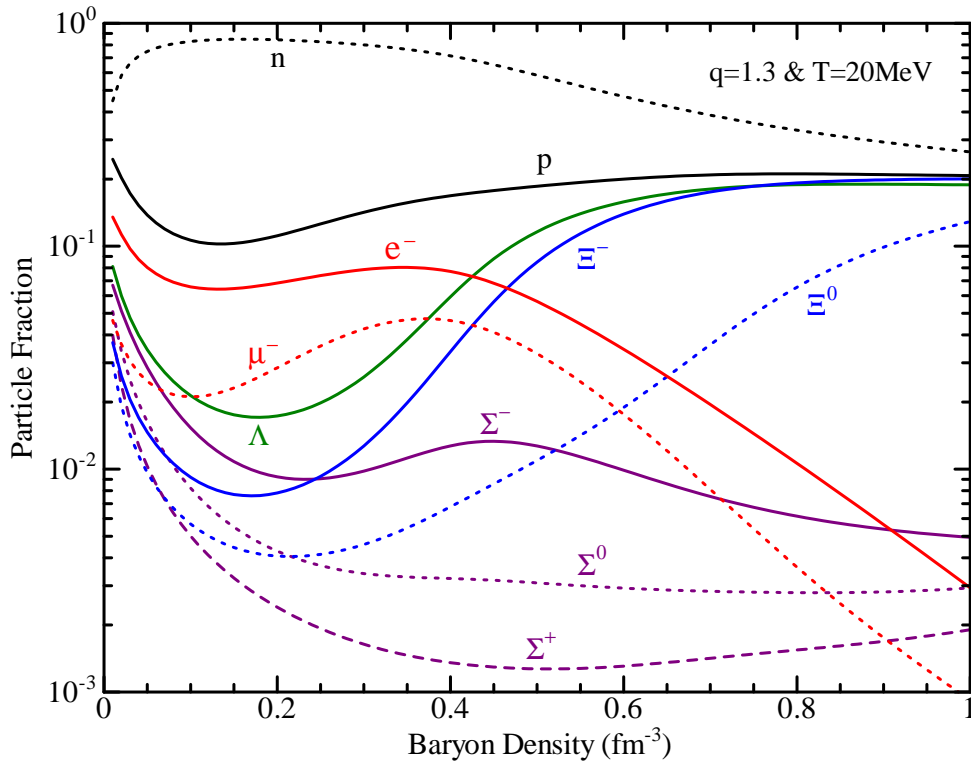


Figure 2: The particle fractions in the core of hot NS at $T = 20 \text{ MeV}$ in the generalized thermo-statistics of the power-law index $q = 1.1$


 Figure 3: The same as Fig. 2 but for $q = 1.2$

 Figure 4: The same as Fig. 2 but for $q = 1.3$

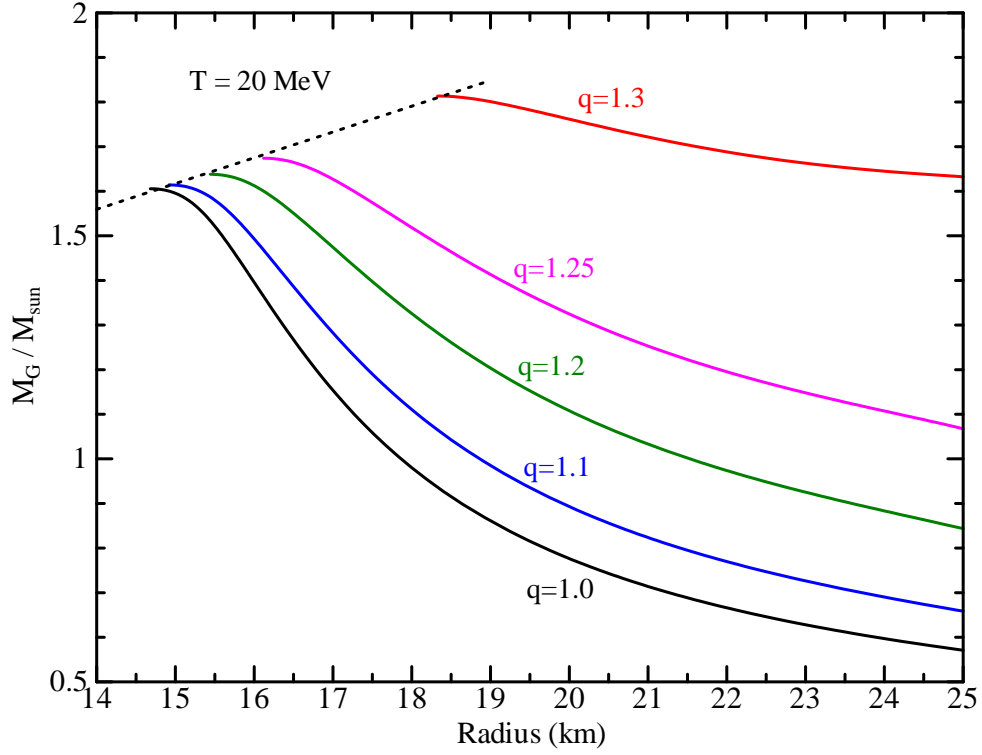


Figure 5: The gravitational masses of NSs as functions of their radii at $T = 20\text{MeV}$ from $q = 1.0$ to 1.3.

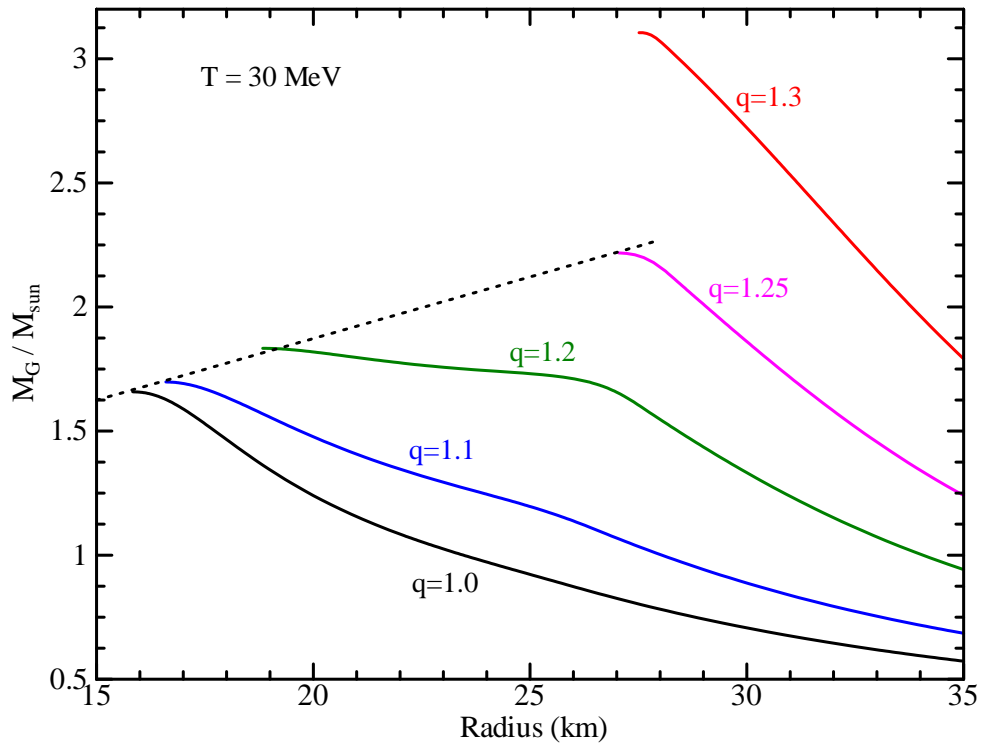


Figure 6: The same as Fig. 5 but at $T = 30\text{MeV}$.